Lie group analysis for the effects of chemical reaction on MHD stagnation-point flow of heat and mass transfer towards a heated porous stretching sheet with suction or injection

Ahmed A. Afify[1,2], **Nasser S. Elgazery**[1,3]

[1]Department of Mathematics, Deanship of Educational Services, Qassim University
P.O. Box 6595, Buraidah: 51452 Saudi Arabia

[2]Department of Mathematics, Faculty of Science, Helwan University
Ain Helwan, P.O. Box 11795, Cairo, Egypt
afify65@yahoo.com

[3]Department of Mathematics, Faculty of Education, Ain Shams University
Roxy, Heliopolis, Cairo, Egypt
nasser_522000@yahoo.com

Received: 6 October, 2010 / **Revised:** 13 December 2011 / **Published online:** 24 February 2012

Abstract. An analysis is carried out to study two dimensional stagnation-point flow of heat and mass transfer of an incompressible, electrically conducting fluid towards a heated porous stretching sheet embedded in a porous medium in the presence of chemical reaction, heat generation/absorption and suction or injection effects. A scaling group of transformations is applied to the governing equations. After finding three absolute invariants a third order ordinary differential equation corresponding to the momentum equation and two second order ordinary differential equation corresponding to energy and diffusion equations are derived. Furthermore the similarity equations are solved numerically by using shooting technique with fourth-order Runge–Kutta integration scheme. A comparison with known results is excellent. The phenomenon of stagnation-point flow towards a heated porous stretching sheet in the presence of chemical reaction, suction or injection with heat generation/absorption effects play an important role on MHD heat and mass transfer boundary layer. The results thus obtained are presented graphically and discussed.

Keywords: MHD, similarity solutions, stagnation-point, chemical reaction, suction/injection, heat generation/absorption, porous medium.

1 Introduction

The theoretical study of magnetohydrodynamic (MHD) has been a subject of great interest due to its widespread applications in designing cooling systems which are liquid metals, MHD generators, accelerators, pumps and flow meters. Furthermore the continuous surface heat and mass transfer problem has many practical applications in electro-chemistry and polymer processing. Various aspects of this problem have been studied by some

researchers (Chakrabarti and Gupta, [1]; Gupta and Gupta, [2]; Sakiadis, [3–5]). Most studies have been concerned with constant surface velocity. In nature, the presence of pure air or water is impossible. Some foreign mass may be present either naturally or mixed with air or water. The equations of motion for gas or water flow, taking into account the presence of foreign mass of low level were derived by Gebhart [6] and the effect of the presence of foreign mass on the free convection flow past a semi infinite vertical plate were studied by Gebhart and Pera [7]. Furthermore, the presence of foreign mass in air or water is caused by some kind of chemical reaction. During chemical reaction between two species, heat is also generated. Elperin and Fominykh [8] discussed the exact analytical solution of a convective diffusion from a wedge to a flow with a first order chemical reaction at the surface. The effects of mass transfer on flow past an impulsively started infinite vertical plate with constant heat flux and chemical reaction were studied by Das et al. [9]. Recently, Chiam [10] studied two-dimensional steady stagnation-point flow of an incompressible viscous fluid towards a stretching surface. Mahapatra and Gupta [11] studied two-dimensional stagnation-point flow of an incompressible viscous electrically conducting fluid towards a stretching surface. Mahapatra et al. [12] studied two-dimensional stagnation-point flow of an incompressible viscous electrically conducting power-law fluid over a stretching surface. Mahapatra and Gupta [13] studied the steady two dimensional stagnation-point flow and heat transfer characteristics over a stretching sheet. Lie group analysis, also called symmetry analysis was developed by Sophius Lie to find point transformations which map a given differential equation to it self. This method unifies almost all known exact integration techniques for both ordinary and partial differential equations Oberlack [14]. In the field of fluid mechanics, most of the researchers try to obtain the similarity solutions in such cases. In case of scaling group of transformations, the group-invariant solutions known similarity solutions, Pakdemirli and Yurusoy [15]. Lie group of transformations theory is used in this paper to find out the symmetries of the problem and then to study which of them are appropriate to provide group-invariant or more specifically similarity solutions. This method applied intensively by some researchers [16–22]. In this paper, we discuss a steady two dimensional stagnation-point flow of heat and mass transfer over a heated porous stretching sheet embedded in a porous medium in the presence of a chemical reaction, suction or injection with heat generation/absorption effects. By applying the scaling group transformations, the set of governing equations and the boundary conditions are reduced to non-linear ordinary differential equations with appropriate boundary conditions. Finally, the similarity equations are solved numerically by using shooting technique with fourth-order Runge–Kutta integration scheme.

2 Governing equations

Consider the two-dimensional steady of the stagnation-point flow of heat and mass transfer of an incompressible, electrically conducting fluid over a stretching sheet coinciding with the plane $\bar{y} = 0$. Two equal and opposite forces are applied along the $\bar{x}$-axis so that the surface stretched keeping the origin fixed, as shown in Fig. 1. The uniform transverse

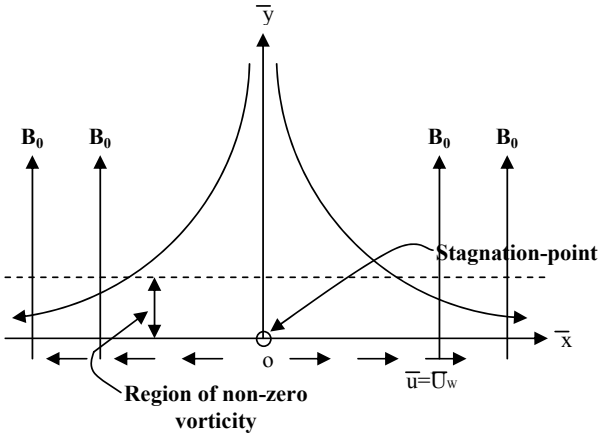

Fig. 1. A sketch of the physical problem.

magnetic field B_0 is imposed along the $\bar{y}$-axis. The induced magnetic field is neglected as the magnetic Reynolds number of the flow is taken to be very small. It is also assumed that the external electric field is zero and the electric field due to polarization of charges is negligible. The temperature and the concentration of the ambient fluid are T_∞ and C_∞, and those at the stretching surface are T_w and C_w respectively. It is also assumed that the viscous and electrical dissipation are neglected. The MHD equations for two dimensional stagnation-point flow of heat and mass transfer boundary layer towards a heated porous stretching sheet are [11]:

$$\frac{\partial \bar{u}}{\partial \bar{x}} + \frac{\partial \bar{v}}{\partial \bar{y}} = 0, \tag{1}$$

$$\bar{u}\frac{\partial \bar{u}}{\partial \bar{x}} + \bar{v}\frac{\partial \bar{u}}{\partial \bar{y}} = \bar{U}_e\frac{\partial \bar{U}_e}{\partial \bar{x}} + \nu\frac{\partial^2 \bar{u}}{\partial \bar{y}^2} + \frac{\sigma B_0^2}{\rho}(\bar{U}_e - \bar{u}) + \frac{\nu\tau}{k}(\bar{U}_e - \bar{u}), \tag{2}$$

$$\bar{u}\frac{\partial \bar{T}}{\partial \bar{x}} + \bar{v}\frac{\partial \bar{T}}{\partial \bar{y}} = \alpha\frac{\partial^2 \bar{T}}{\partial \bar{y}^2} + \frac{Q_0}{\rho C_P}(\bar{T} - \bar{T}_\infty), \tag{3}$$

$$\bar{u}\frac{\partial \bar{C}}{\partial \bar{x}} + \bar{v}\frac{\partial \bar{C}}{\partial \bar{y}} = D\frac{\partial^2 \bar{C}}{\partial \bar{y}^2} - k_0(\bar{C} - \bar{C}_\infty)^n. \tag{4}$$

The boundary conditions for Eqs. (1)–(4) are expressed as:

$$\begin{aligned} &\bar{u} = \bar{U}_w(\bar{x}) = C_1\bar{x}, \quad \bar{v} = \bar{v}_w(\bar{x}), \quad \bar{T} = \bar{T}_w, \quad \bar{C} = \bar{C}_w \quad \text{at } \bar{y} = 0, \\ &\bar{u} = \bar{U}_e(\bar{x}) \to a\bar{x}, \quad \bar{T} \to \bar{T}_\infty, \quad \bar{C} \to \bar{C}_\infty \qquad\qquad\quad \text{as } \bar{y} \to \infty, \end{aligned} \tag{5}$$

where $\bar{u}$, $\bar{v}$ are the velocity components in the $\bar{x}$ and $\bar{y}$ directions respectively, ν is the kinematic viscosity, σ is the electrical conductivity, ρ is the density of the fluid, $\bar{T}$ and $\bar{T}_\infty$ are the temperature of the fluid inside the thermal boundary layer and the fluid temperature in the free stream, respectively, while $\bar{C}$ and $\bar{C}_\infty$ are the corresponding concentrations.

Also, C_1 and a are positive constants, $\bar{U}_w(\bar{x})$ is the stretching velocity, $\bar{U}_e(\bar{x})$ is the stagnation point velocity, $\bar{v}_w$ is a transpiration velocity through the porous surface, C_P is the specific heat at constant pressure, α is the thermal diffusity, k is the permeability of the porous medium, k_0 is the reaction rate constant, n order of reaction and D is the diffusion coefficient. We introduced the following dimensionless quantities:

$$\begin{aligned} &x = \frac{C_1\bar{x}}{U_1}, \quad y = \sqrt{\frac{C_1}{\nu}}\bar{y}, \quad u = \frac{\bar{u}}{U_1}, \quad v = \frac{\bar{v}}{\sqrt{C_1\nu}}, \\ &U_e = \frac{\bar{U}_e}{U_1}, \quad \theta = \frac{\bar{T}-\bar{T}_\infty}{\bar{T}_w-\bar{T}_\infty}, \quad \phi = \frac{\bar{C}-\bar{C}_\infty}{\bar{C}_w-\bar{C}_\infty}, \end{aligned} \tag{6}$$

where U_1 is the characteristic velocity. Substitution from Eq. (6) into Eqs. (1)–(4) and boundary conditions (5), gives

$$\frac{\partial u}{\partial x} + \frac{\partial v}{\partial y} = 0, \tag{7}$$

$$u\frac{\partial u}{\partial x} + v\frac{\partial u}{\partial y} = U_e\frac{\partial U_e}{\partial x} + \frac{\partial^2 u}{\partial y^2} + M^2(U_e-u) + k_1(U_e-u), \tag{8}$$

$$u\frac{\partial \theta}{\partial x} + v\frac{\partial \theta}{\partial y} = \frac{1}{Pr}\frac{\partial^2 \theta}{\partial y^2} + \beta\theta, \tag{9}$$

$$u\frac{\partial \phi}{\partial x} + v\frac{\partial \phi}{\partial y} = \frac{1}{Sc}\frac{\partial^2 \phi}{\partial y^2} - \gamma\phi^n, \tag{10}$$

$$\begin{aligned} &u = x, \quad v = \frac{v_w}{\sqrt{C_1\nu}}, \quad \theta = 1, \quad \phi = 1 \quad \text{at } y = 0, \\ &u \to \lambda x, \quad \theta \to 0, \quad \phi \to 0 \quad \text{as } y \to \infty. \end{aligned} \tag{11}$$

From the continuity equation (7), there exists a stream function $\psi(x,y)$ such that

$$u = \frac{\partial \psi}{\partial y}, \quad v = -\frac{\partial \psi}{\partial x}, \tag{12}$$

which satisfies Eq. (7) identically. Substitution from Eq. (12) into Eqs. (7)–(10) and (11), gives

$$\psi_y\psi_{xy} - \psi_x\psi_{yy} - U_e\frac{\partial U_e}{\partial x} - \psi_{yyy} - k_1(U_e-\psi_y) - M^2(U_e-\psi_y) = 0, \tag{13}$$

$$\psi_y\theta_x - \psi_x\theta_y - \frac{1}{Pr}\theta_{yy} - \beta\theta = 0, \tag{14}$$

$$\psi_y\phi_x - \psi_x\phi_y - \frac{1}{Sc}\phi_{yy} + \gamma\phi^n = 0, \tag{15}$$

$$\begin{aligned} &\psi_y = x, \quad \psi_x = -\frac{v_w}{\sqrt{C_1\nu}}, \quad \theta = 1, \quad \phi = 1 \quad \text{at } y = 0, \\ &\psi_y \to \lambda x, \quad \theta \to 0, \quad \phi \to 0 \quad \text{as } y \to \infty. \end{aligned} \tag{16}$$

3 Scaling group of transformations

We now introduce the simplified form of Lie group transformations namely, the scaling group of transformations [23]:

$$\Gamma\colon\ \begin{cases} x^* = xe^{\epsilon\alpha_1}, \quad y^* = ye^{\epsilon\alpha_2}, \psi^* = \psi e^{\epsilon\alpha_3}, \quad u^* = ue^{\epsilon\alpha_4}, \\ v^* = ve^{\epsilon\alpha_5}, \quad {U_e}^* = U_e e^{\epsilon\alpha_6}, \quad \theta^* = \theta e^{\epsilon\alpha_7}, \quad \phi^* = \phi e^{\epsilon\alpha_8}. \end{cases} \tag{17}$$

Equation (17) may be considered as a point-transformation which transforms coordinates $(x, y, \psi, u, v, U_e, \theta, \phi)$ to the coordinates $(x^*, y^*, \psi^*, u^*, v^*, U_e^*, \theta^*, \phi^*)$, substituting (17) in Eqs. (13)–(15) and boundary conditions (16), we get

$$e^{\epsilon(\alpha_1+2\alpha_2-2\alpha_3)}\big(\psi^*_{y^*}\psi^*_{x^*y^*} - \psi^*_{x^*}\psi^*_{y^*y^*}\big) - e^{\epsilon(\alpha_2-2\alpha_6)}U^*_e\frac{\partial U^*_e}{\partial x^*} - e^{\epsilon(3\alpha_2-\alpha_3)}\psi^*_{y^*y^*y^*} - k_1\big(e^{-\epsilon\alpha_6}U^*_e - e^{\epsilon(\alpha_2-\alpha_3)}\psi^*_{y^*}\big) - M^2\big(e^{-\epsilon\alpha_6}U^*_e - e^{\epsilon(\alpha_2-\alpha_3)}\psi^*_{y^*}\big) = 0, \tag{18}$$

$$e^{\epsilon(\alpha_1+\alpha_2-\alpha_3-\alpha_7)}\big(\psi^*_{y^*}\theta^*_{x^*} - \psi^*_{x^*}\theta^*_{y^*}\big) - \frac{1}{Pr}e^{\epsilon(2\alpha_2-\alpha_7)}\theta^*_{y^*y^*} - \beta e^{-\epsilon\alpha_7}\theta^* = 0, \tag{19}$$

$$e^{\epsilon(\alpha_1+\alpha_2-\alpha_3-\alpha_8)}\big(\psi^*_{y^*}\phi^*_{x^*} - \psi^*_{x^*}\phi^*_{y^*}\big) - \frac{1}{Sc}e^{\epsilon(2\alpha_2-\alpha_8)}\phi^*_{y^*y^*} + \gamma e^{-\epsilon n\alpha_8}\phi^{*n} = 0, \tag{20}$$

$$\begin{aligned} &e^{\epsilon(\alpha_2-\alpha_3)}\psi^*_{y^*} = e^{-\epsilon\alpha_1}x^*, \quad e^{\epsilon(\alpha_1-\alpha_3)}\psi^*_{x^*} = -\frac{v_w}{\sqrt{C_1\nu}}, \\ &\quad \theta^* = 1, \quad \phi^* = 1 && \text{at } y^* = 0, \\ &e^{\epsilon(\alpha_2-\alpha_3)}\psi^*_{y^*} \to \lambda e^{-\epsilon\alpha_1}x^*, \quad \theta^* \to 0, \quad \phi^* \to 0 && \text{as } y^* \to \infty. \end{aligned} \tag{21}$$

The system will remain invariant under the group of transformations Γ; we would have the following relations among the parameters, namely

$$\begin{aligned} &\alpha_1 + 2\alpha_2 - 2\alpha_3 = \alpha_2 - 2\alpha_6 = 3\alpha_2 - \alpha_3 = -\alpha_6 = \alpha_2 - \alpha_3, \\ &\alpha_1 + \alpha_2 - \alpha_3 - \alpha_7 = \alpha_2 - 2\alpha_6 = 2\alpha_2 - \alpha_7 = \alpha_7, \\ &\alpha_1 + \alpha_2 - \alpha_3 - \alpha_8 = 2\alpha_2 - \alpha_8 = -n\alpha_8. \end{aligned} \tag{22}$$

By solving the previous conditions with boundary conditions, we obtain

$$\alpha_1 = \alpha_3 = \alpha_4 = \alpha_6 \quad \text{and} \quad \alpha_2 = \alpha_5 = \alpha_7 = \alpha_8 = 0. \tag{23}$$

The set of transformations Γ reduces to

$$\Gamma\colon\ \begin{cases} x^* = xe^{\epsilon\alpha_1}, \quad y^* = y, \quad \psi^* = \psi e^{\epsilon\alpha_1}, \quad u^* = ue^{\epsilon\alpha_1}, \\ v^* = v, {U_e}^* = U_e e^{\epsilon\alpha_1}, \quad \theta^* = \theta, \quad \phi^* = \phi. \end{cases} \tag{24}$$

Expanding by Taylor's method in powers of ϵ and keeping terms up to the order ϵ, we get

$$\Gamma\colon\ \begin{cases} x^* - x = x\epsilon\alpha_1, \quad \psi^* - \psi = \psi\epsilon\alpha_1, u^* - u = u\epsilon\alpha_1, {U_e}^* - U_e = U_e\epsilon\alpha_1, \\ y^* - y = v^* - v = \theta^* - \theta = \phi^* - \phi = 0. \end{cases} \tag{25}$$

In terms of differentials these yield

$$\frac{\mathrm{d}x}{\alpha_1 x} = \frac{\mathrm{d}y}{0} = \frac{\mathrm{d}\psi}{\alpha_1 \psi} = \frac{\mathrm{d}u}{\alpha_1 u} = \frac{\mathrm{d}U_e}{\alpha_1 U_e} = \frac{\mathrm{d}v}{0} = \frac{\mathrm{d}\theta}{0} = \frac{\mathrm{d}\phi}{0}. \tag{26}$$

Solving the above equations, we get

$$y^* = \eta, \psi^* = x^* f(\eta), \quad {U_e}^* = \lambda x^*, \quad \theta^* = \theta(\eta), \quad \phi^* = \phi(\eta). \tag{27}$$

With the help of these relations, Eqs. (18)–(20) and boundary conditions (21), become

$$f''' + ff'' - f'^2 + \big(k_1 + M^2\big)\big(\lambda - f'^2\big) + \lambda^2 = 0, \tag{28}$$

$$\theta'' + Pr\big(f\theta' + \beta\theta\big) = 0, \tag{29}$$

$$\phi'' + Sc\big(f\phi' - \gamma\phi^n\big) = 0. \tag{30}$$

With boundary conditions:

$$\begin{aligned} &f = S, \quad f' = 1, \quad \theta = 1, \quad \phi = 1 \quad && \text{at } \eta = 0, \\ &f' \to \lambda, \quad \theta \to 0, \quad \phi \to 0 && \text{as } \eta \to \infty, \end{aligned} \tag{31}$$

where primes denote differentiation with respect to η, $M = B_0\sqrt{\sigma/\rho C_1}$ is the Hartmann number, $k_1 = \nu\tau/(kC_1)$ is porosity parameter, $\lambda = a/C_1$ is the velocity parameter, $Pr = \nu/\alpha$ is the Prandtl number, $\beta = Q_0/(\rho C_1 C_P)$ is the heat source or sink parameter, $Sc = \nu/D$ is the Schmidt number, $\gamma = (k_0/C_1)(C_w - C_\infty)$ is the chemical reaction parameter, $S = -v_w/\sqrt{\nu C_1}$ is the suction or injection parameter. The quantities of physical interest in this problem are the local skin friction coefficient, the local Nusselt number, and the local Sherwood numbers, which are defined by:

$$C_f Re_x = f''(0), \quad Nu = -\theta'(0), \quad Sh = -\phi'(0). \tag{32}$$

4 Numerical method for solution

Equations (28)–(30) constitute a highly non-linear coupled boundary value problem of third and second order, which closed-form solution cannot be obtained. Hence the problem has been solved numerically using a shooting technique along with fourth order Runge–Kutta integration. The basic idea of the shooting method for solving boundary value problem is to try to find appropriate initial condition for which the computed solution "hits the target" so that the boundary conditions at the other points are satisfied. Furthermore, the higher order non-linear differential equations are converted into simultaneous linear differential equations of first order and they are further transformed into initial valued problem applying the shooting method incorporating fourth order Runge–Kutta method. The iterative solution procedure was carried out until the error in the solution became less than a predefined tolerance level. So we develop most effective numerical shooting technique with fourth-order Runge–Kutta integration algorithm. To select η_∞

we begin with some initial guess value and solve the problem with some particular set of parameters to obtain $f''(0)$, $\theta'(0)$ and $\phi'(0)$. The solution process is repeated with another larger value of η_∞ until two successive values of $f''(0)$, $\theta'(0)$ and $\phi'(0)$ differ only after desired digit signifying the limit of the boundary along η. The last value of η_∞ is chosen as appropriate value for that particular set of parameters. Equations (28)–(30) of third order in f and second order in θ and ϕ has been reduced to a system of seven simultaneous equations of first order for seven unknowns following the method of superposition [24]. To solve this system we require seven initial conditions whilst we have only two initial conditions $f'(0)$ and $f(0)$ on f, two initial conditions on each θ and ϕ. Still there are three initial conditions $f''(0)$, $\theta'(0)$ and $\phi'(0)$ which are not prescribed. Now, we employ numerical shooting technique where these two ending boundary conditions are utilized to produce two known initial conditions at $\eta = 0$. The computer program of the numerical method was executed in MATHEMATICA 7^{TM} running on a PC.

5 Results and discussion

By using a scaling group of transformations to analysis of the governing equations and the boundary conditions, the two independent variables are reduced by one consequently the governing equations reduce to a system of non-linear ordinary differential equations with the appropriate boundary conditions. Finally the system of similarity Eqs. (28)–(30) with boundary conditions (31) are solved numerically by employing shooting technique with fourth-order Runge–Kutta integration algorithm similar to that described by Na [24]. In order to get a clear insight of the physical problem, the velocity f', the temperature θ and the concentration ϕ have been discussed by assigning numerical values to the parameters encountered in the problem. To be realistic, the values of Hartmann number M takes values $0, 1, 2, 3$, porosity parameter k_1 takes values from 0 to10, the velocity parameter λ takes values 0.1 to 50 the chemical reaction parameter γ takes values $0.5, 1, 1.5, 2, 3$, order of reaction n takes values $1, 3$, heat source or sink parameter β takes values $0, \pm1, \pm2, \pm3$, suction or injection parameter S takes values $0, \pm0.5, \pm1$ with Prandtl number Pr takes value $0.72, 1, 7$ and Schmidt number Sc takes value 0.62. Comparison with previously published data available in the literature as well as the exact solution for some particular cases shows a good agreement [25]. The comparison is shown in Table 1.

Table 1. Values of $f(0)$ for different values of η at $S = M = k_1 = \lambda = 0$.

	$f(0)$		
η	Exact solution [25]	Present results	The error
0.00	0	-1.58819×10^{-21}	1.58819×10^{-21}
0.01	0.00995017	0.0099501	6.87806×10^{-8}
0.02	0.0198013	0.019801	2.97751×10^{-7}
0.03	0.0295545	0.0295538	6.46904×10^{-7}
0.04	0.0392106	0.0392094	1.13578×10^{-6}
0.05	0.0487706	0.0487688	1.76447×10^{-6}
0.10	0.0951626	0.0951556	7.00387×10^{-6}

In order to assess the accuracy of the numerical method, we have compared our local skin friction with the previously published work [26], and [27]. The comparison is shown in Table 2 and a good agreement was observed. From Table 3, it is observed that the local Nusselt number, $\theta'(0)$, increases with an increase in Prandtl number Pr, while it decreases with an increase in heat source or sink parameter β. Table 4; exhibit the behavior of the skin friction coefficient, $f''(0)$, the local Nusselt number, $-\theta'(0)$, and the local Sherwood number, $-\phi'(0)$, for different values of Hartmann number, M, and suction or injection parameter S. It is observed that the skin friction coefficient, $f''(0)$, increases with an increase in Hartmann number, M, and suction or injection parameter S. The local Nusselt number, $-\theta'(0)$, and the local Sherwood number, $-\phi'(0)$, increase with an increase suction or injection parameter, S, and decrease with an increase in Hartmann number M. Table 5; exhibit the behavior the local Nusselt number, $-\theta'(0)$, and the local Sherwood number, $-\phi'(0)$, for different values of porosity parameter k_1 and the velocity parameter λ. It is observed that the local Nusselt number, $-\theta'(0)$, and the local Sherwood number, $-\phi'(0)$, decrease with an increase porosity parameter k_1 for a fixed value of λ with $\lambda < 1$, and the opposite is observed when $\lambda > 1$. Finally, for a fixed value of k_1 both the local Nusselt number, $-\theta'(0)$, and the local Sherwood number, $-\phi'(0)$, increase with an increase in velocity parameter λ.

Table 2. Values of $f''(0)$ for different values of λ at $S = M = k_1 = 0$.

λ	$f''(0)$		
	Mahapatra and Gupta [26]	Nazer et al. [27]	Present results
0.01		−0.9980	−0.999198
0.02		−0.9958	−0.996774
0.05		−0.9876	−0.988181
0.10	−0.9694	−0.9694	−0.969656
0.20	−0.9181	−0.9181	−0.918165
0.50	−0.6673	−0.6673	−0.667264
2.00	2.0175	2.0176	2.0175
3.00	4.7293	4.7296	4.72928
5.00		11.7537	11.752
10.00		36.2687	36.2574
20.00		106.5744	106.507
50.00		430.6647	429.978

Table 3. Values of $-\theta'(0)$ for different values of β and Pr at $S = M = 0.5$, $k_1 = 0.1$ and $\lambda = 0.5$.

β	$-\theta'(0)$		
	$Pr = 0.72$	$Pr = 1.0$	$Pr = 7.0$
−0.2	0.912228	1.13883	4.84100
−0.1	0.864310	1.08425	4.73428
0.0	0.813516	1.02659	4.62437
0.1	0.759348	0.965375	4.51101
0.2	0.701169	0.899961	4.39389

Table 4. Values of $f''(0)$, $-\theta'(0)$ and $-\phi'(0)$ for different values of S and M at $\lambda = k_1 = \beta = 0.1$, $\gamma = n = 1$, $Sc = 0.62$ and $Pr = 0.72$.

M	$f''(0)$		
	$S = -0.5$	$S = 0.0$	$S = 0.5$
0.0	−0.805237	−1.01007	−1.26387
0.1	−0.809136	−1.01403	−1.26771
0.2	−0.820748	−1.02582	−1.27916
0.3	−0.839834	−1.04520	−1.29798
0.4	−0.866018	−1.07176	−1.32381
0.5	−0.898818	−1.10501	−1.35620
1.0	−1.142390	−1.35135	−1.59740

M	$-\theta'(0)$		
	$S = -0.5$	$S = 0.0$	$S = 0.5$
0.0	0.209905	0.410648	0.664261
0.1	0.209222	0.410058	0.663836
0.2	0.207199	0.408311	0.662576
0.3	0.203917	0.405471	0.660523
0.4	0.199503	0.401638	0.657744
0.5	0.194120	0.396940	0.654321
1.0	0.159222	0.365586	0.630923

M	$-\phi'(0)$		
	$S = -0.5$	$S = 0.0$	$S = 0.5$
0.0	0.764387	0.916936	1.09287
0.1	0.764208	0.916764	1.09272
0.2	0.763679	0.916254	1.09228
0.3	0.762820	0.915426	1.09156
0.4	0.761662	0.914307	1.09059
0.5	0.760244	0.912935	1.08939
1.0	0.750779	0.903681	1.08116

Table 5. Values of $-\theta'(0)$ and $-\phi'(0)$ for different values of k_1 and λ at $S = M = 0.5$, $\beta = 0.1$, $\gamma = n = 1$, $Sc = 0.62$ and $Pr = 0.72$.

k_1	$-\theta'(0)$			
	$\lambda = 0.1$	$\lambda = 0.5$	$\lambda = 2.0$	$\lambda = 3.0$
0.0	0.658134	0.767954	1.05237	1.19442
0.1	0.654321	0.766953	1.05291	1.19510
0.2	0.650702	0.765988	1.05344	1.19577
0.3	0.647261	0.765058	1.05397	1.19642
0.4	0.643982	0.764159	1.05448	1.19707
0.5	0.640854	0.763291	1.05499	1.19771
1.0	0.627085	0.759348	1.05739	1.20078
	$-\phi'(0)$			
	$\lambda = 0.1$	$\lambda = 0.5$	$\lambda = 2.0$	$\lambda = 3.0$
0.0	1.09073	1.12514	1.27433	1.36984
0.1	1.08939	1.12466	1.27469	1.37033
0.2	1.08812	1.12420	1.27505	1.37082
0.3	1.08692	1.12376	1.27541	1.37130
0.4	1.08576	1.12333	1.27575	1.37177
0.5	1.08466	1.12292	1.27610	1.37223
1.0	1.07980	1.12102	1.27772	1.37448

From Table 6, it is observed that the local Sherwood number, $-\phi'(0)$, increases with an increase chemical reaction parameter γ while it decreases with an increase in order of reaction n.

Table 6. Values of $-\phi'(0)$ for different values of γ at $k_1 = 0.1$, $S = M = 0.5$, $Sc = 0.62$ and $\lambda = 0.5$.

	$-\phi'(0)$		
γ	$n = 1$	$n = 2$	$n = 3$
0.5	0.948328	0.871389	0.835834
1.0	1.12102	0.990965	0.927534
1.5	1.26868	1.097750	1.011240
2.0	1.39952	1.195000	1.088670
3.0	1.62733	2.298860	1.229150

Figures 2, 3, and 4 depict the velocity, the temperature, and the concentration profiles for different values of Hartmann number M and velocity parameter λ. Figure 2, show that for a fixed value of λ with $\lambda < 1$, the velocity at a point decreases with increase in the Hartmann number M. This can be explained physically as follows. As the strength of the magnetic field characterized by M increases, the Lorentz force which opposes the flow in the boundary layer also increases and leads to enhanced deceleration of the flow. On the other hand for a fixed value of λ with $\lambda > 1$, the velocity at a point increases with increase in M. This paradoxical result can be explained by the fact that when $\lambda < 1$, the velocity of the stretching sheet exceeds the velocity of the inviscid stream and an inverted boundary layer is formed near the surface. Figures 3 and 4 show that the temperature and the concentration profiles increase with an increase in Hartmann number M. The effects of a transverse magnetic field on an electrically conducting fluid gives rise to a resistive-type force called the Lorentz force. This force increases its temperature and concentration boundary layers. On the contrary, the temperature and the concentration

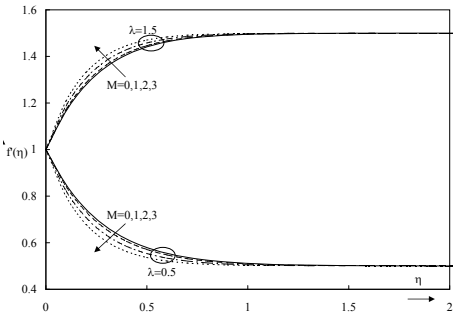

Fig. 2. Variation of $f'(\eta)$ with η for several values of M when $\lambda = 0.5$ and 1.5 for $S = 3$ and $k_1 = 0.1$.

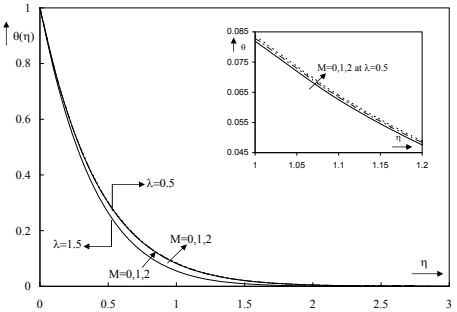

Fig. 3. Variation of $\theta(\eta)$ with η for several values of M when $\lambda = 0.5$ and 1.5 for $Pr = 0.72$, $\beta = 0.1$, $S = 3$ and $k_1 = 0.1$ (the inset show a zoom of curve).

profiles decrease with an increase of velocity parameter λ. Figure 5, shows that for a fixed value of λ with $\lambda < 1$, the velocity at a point decreases with increase in porosity parameter k_1. That is because, $\lambda < 1$ for an increase k_1 causes an increase in boundary layer thickness and as a result a decrease in the velocity. On the other hand for a fixed value of λ with $\lambda > 1$, the velocity at a point increases with increase in porosity parameter k_1. That is because, for $\lambda > 1$ an increase k_1 causes a decrease in boundary layer thickness and as a result an increase in the velocity. Also, it is observed that the temperature and concentration profiles are not sensitive with increase of porosity parameter k_1 and velocity parameter λ. Figures 6(a), 6(b), 7, and 8 depict the velocity, the temperature, and the concentration profiles for different values of velocity parameter λ and suction or injection parameter S. Figures 6(a), 6(b), show that for a fixed value of λ with $\lambda < 1$, the velocity at a point decreases with increase in the suction or injection parameter S, and the opposite is observed when $\lambda > 1$.

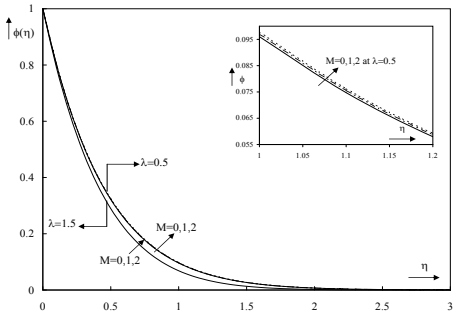

Fig. 4. Variation of $\phi(\eta)$ with η for several values of M when $\lambda = 0.5$ and 1.5 for $Sc = 0.62$, $\gamma = 0.5$, $n = 1$, $S = 3$ and $k_1 = 0.1$ (the inset show a zoom of curve).

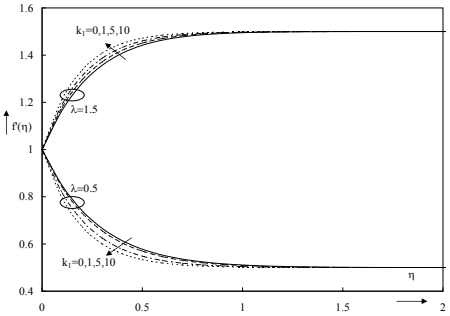

Fig. 5. Variation of $f'(\eta)$ with η for several values of k_1 when $\lambda = 0.5$ and 1.5 for $S = 3$ and $M = 0.5$.

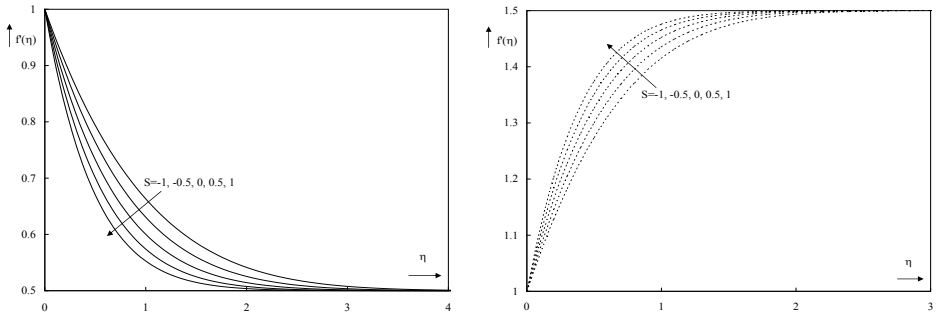

(a) (b)

Fig. 6. Variation of $f'(\eta)$ with η for several values of S for $k_1 = 0.1$ and $M = 0.5$ when (a) $\lambda = 0.5$ and (b) $\lambda = 1.5$.

Figures 7 and 8 show that the temperature and the concentration profiles decrease with an increase in velocity parameter λ and suction or injection parameter S. Figure 9 shows that the temperature profiles increase with an increase in heat source or sink parameter β. Also, it is observed that the velocity and concentration profiles are not sensitive with an increase in heat source or sink parameter β. Figure 10, shows that the concentration profiles increase with an increase in order of reaction n while it decreases with an increase in chemical reaction parameter γ. Also, it is observed that the velocity and temperature profiles are not sensitive with an increase in chemical reaction parameter γ and order of reaction n.

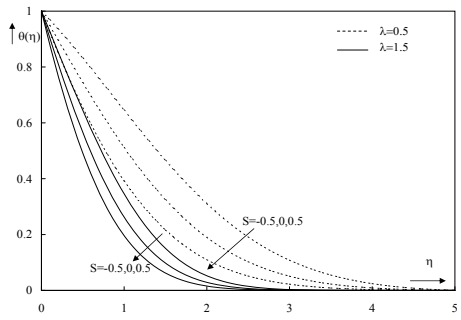

Fig. 7. Variation of $\theta(\eta)$ with η for several values of S when $\lambda = 0.5$ and 1.5 for $Pr = 0.72$, $\beta = 0.1$, $M = 0.5$ and $k_1 = 0.1$.

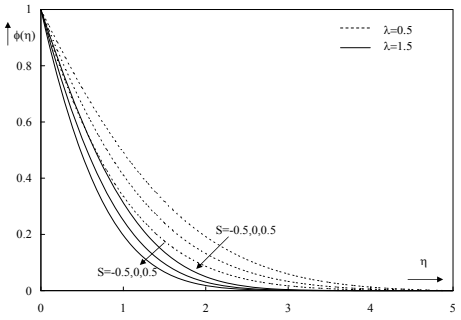

Fig. 8. Variation of $\phi(\eta)$ with η for several values of S when $\lambda = 0.5$ and 1.5 for $Sc = 0.62$, $\gamma = 0.5$, $n = 1$, $S = 3$ and $k_1 = 0.1$.

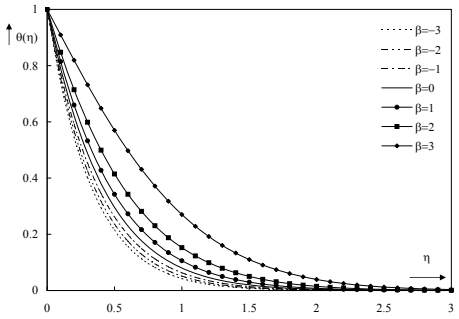

Fig. 9. Variation of $\theta(\eta)$ with η for several values of β for $\lambda = 0.5$, $Pr = 0.72$, $S = 3$, $M = 0.5$ and $k_1 = 0.1$.

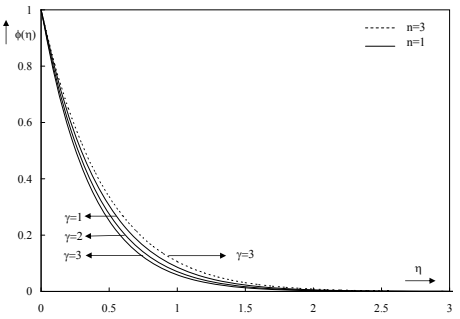

Fig. 10. Variation of $\phi(\eta)$ with η for several values of γ when $n=1$ and 3 for $Sc=0.62$, $\lambda = 0.5$, $M = 0.5$, $S = 3$ and $k_1 = 0.1$.

6 Conclusions

The present work helps us understanding numerically as well as physically the stagnation-point phenomenon on heat and mass transfer flow of an incompressible, electrically con-

ducting fluid towards a heated porous stretching sheet embedded in a porous medium in the presence of chemical reaction, heat generation/absorption and suction or injection effects. The similarity solutions are obtained using scaling transformations. The set of governing equations and the boundary condition are reduced to ordinary differential equations with appropriate boundary conditions. Furthermore the similarity equations are solved numerically by using shooting technique with fourth-order Runge–Kutta integration scheme. A comparison with previously published work is performed and the results are found to be in good agreement. Based on the obtained results, the following conclusions may be drawn:

(i) The local Nusselt number increases with an increase in Prandtl number Pr, while it decreases with an increase in heat source or sink parameter β.

(ii) The skin friction coefficient increases while the local Nusselt number and the local Sherwood number decrease with an increase in Hartmann number M.

(iii) The skin friction coefficient, the local Nusselt number, and the local Sherwood number increase with an increase in suction or injection parameter S.

(iv) The local Nusselt number and the local Sherwood number decrease with an increase porosity parameter k_1 for $\lambda < 1$, and the opposite are observed when $\lambda > 1$.

(v) The local Sherwood number increases with an increase chemical reaction parameter γ while it decreases with an increase in order of reaction n.

(vi) The velocity profiles decreases with increase in the Hartmann number M, porosity parameter k_1 and suction or injection parameter S for $\lambda < 1$, and the opposite is observed when $\lambda > 1$. The temperature and the concentration profiles increase with an increase in Hartmann number M while both of them decrease with an increase in velocity parameter λ and suction or injection parameter S.

(vii) The temperature profiles increase with an increase in heat source or sink parameter β. The concentration profiles increase with an increase in order of reaction n while it decreases with an increase in chemical reaction parameter γ.

Nomenclature

a, C_1	positive constants
B_0	a constant magnetic field
C	concentration of the fluid, $\mathrm{kg\,m^{-2}}$
C_P	specific heat, $\mathrm{J\,kg^{-1}K^{-1}}$
D	Diffusion coefficient of mass, $\mathrm{m^2s^{-1}}$
f'	similarity function
k_0	reaction rate constant
k	permeability of the porous medium
k_1	porosity medium parameter
S	suction or injection parameter
M	Hartmann number
n	order of reaction
Pr	Prandtl number
Re_x	local Reynolds number
Sc	Schmidt number
T	temperature of the fluid, K
$U_w(x)$	stretching velocity of the plate, $\mathrm{m\,s^{-1}}$
$U_e(x)$	stagnation point velocity fluid, $\mathrm{m\,s^{-1}}$
v_w	transpiration velocity through the porous surface, $\mathrm{m\,s^{-1}}$
u, v	the x and y component of the velocity field, $\mathrm{m\,s^{-1}}$
x, y	Cartesian coordinates, m

Greek symbols

ψ	stream function	$\alpha_1, \ldots, \alpha_8$	transformation parameters
η	similarity variable	τ	porosity
θ	dimensionless temperature	σ	electrical conductivity
λ	velocity ratio parameter		
ϕ	dimensionless concentration	*Subscripts*	
ν	kinematic viscosity, $\mathrm{m^2 s^{-1}}$	w	wall condition
γ	chemical reaction parameter	∞	free stream condition
ρ	density, $\mathrm{kg\,m^{-3}}$	o	constant condition
α	thermal diffusity, $\mathrm{m^2 s^{-1}}$		
β	heat source or sink source	*Superscript*	
ϵ	group parameter	$'$	differentiation with respect to η

References

1. A. Chakrabarti, A.S. Gupta, Hydromagnetic flow heat and mass transfer over a stretching sheet, *Q. Appl. Math.*, **33**, pp. 73–78, 1979.

2. P.S. Gupta, A.S. Gupta, Heat and mass transfer on a stretching sheet with suction or blowing, *Can. J. Chem. Eng.*, **55**, pp. 744–746, 1977.

3. B.C. Sakiadis, Boundary-layer behavior on continuous solid surfaces: I. Boundary-layer equations for two dimensional and axisymmetric flow, *AIChE J.*, **7**, pp. 26–28, 1961.

4. B.C. Sakiadis, Boundary-layer behavior on continuous solid surfaces: II. The boundary-layer on a continuous flat surface, *AIChE J.*, **7**, pp. 221–225, 1961.

5. B.C. Sakiadis, Boundary-layer behavior on continuous solid surfaces: III. The boundary-layer on a continuous cylindrical surface, *AIChE J.*, **7**, pp. 467–472, 1961.

6. B. Gebhart, *Heat Transfer*, McGraw Hill, New York, 1971.

7. B. Gebhart, L. Pera, The nature of vertical natural convection flow resulting from the combined buoyancy effects of thermal and mass diffusion, *J. Heat Mass Transfer*, **14**, pp. 2025–2050, 1971.

8. T. Elperin, A. Fominykh, Exact analytical solution of a convective diffusion from a wedge to a flow with a first order chemical reaction at the surface, *Int. Commun. Heat Mass Transfer*, **21**, pp. 227–235, 1994.

9. U.N. Das, R. Deka, V.M. Soundalgekar, Effects of mass transfer on flow past an impulsively started infinite vertical plate with constant heat flux and chemical reaction, *Journal Forschung Im Ingenieurwesen-Engineering Research*, **60**, pp. 284–287. 1994.

10. T.C. Chiam, Stagnation-point flow towards a stretching plate, *J. Phys. Soc. Japan*, **63**, pp. 2443–2444, 1994.

11. T.R. Mahapatra, A.S. Gupta, Magnetohydrodynamic stagnation-point flow towards a stretching sheet, *Acta Mech.*, **152**, pp. 191–196, 2001.

12. T.R. Mahapatra, S.K. Nandy, A.S. Gupta, Magnetohydrodynamic stagnation-point flow of a power-law fluid towards a stretching surface, *Int. J. Non-Linear Mech.*, **44**, pp. 124–129, 2009.

13. T.R. Mahapatra, A.S. Gupta, Heat transfer in stagnation-point flow towards a stretching sheet, *Heat Mass Transfer*, **38**, pp. 517–521, 2002.

14. M. Oberlack, Similarity in non-rotating and rotating turbulent pipe flows, *J. Fluid Mech. differential equations. SIAM Rev.*, **379**, pp. 1–22, 1999.

15. M. Pakdemirli, M. Yurusoy, Similarity transformations for partial differential equations, *SIAM Rev.*, **40**, pp. 96–101, 1998.

16. A.J.A. Morgan, The reduction by one of the number of independent variables in some systems of partial differential equations, *Q. J. Math.*, **3**, pp. 250–259, 1952.

17. M.J. Moran, R.A. Gaggiol, Reduction of the number of variables in systems of partial differential equations with auxiliary conditions, *SIAM J. Appl. Math.*, **16**, pp. 202–215, 1968.

18. S. Sivasankaran, M. Bhuvaneswari, P. Kandaswamy, E.K. Ramasami, Lie group analysis of natural convection heat and mass transfer in an inclined surface, *Nonlinear Anal. Model. Control*, **11**, pp. 201–212, 2006.

19. K. Atalık, Ü. Sönmezler, Symmetry groups and similarity analysis for boundary layer control over a wedge using electric forces, *Int. J. Non-Linear Mech.*, **44**, pp. 883–890, 2009.

20. M. Bhuvaneswari, S. Sivasankaran, M. Ferdows, Lie group analysis of natural convection heat and mass transfer in an inclined surface with chemical reaction, *Nonlinear Anal., Hybrid Syst.*, **3**, pp. 536–542, 2009.

21. A.A. Afify, Similarity solution in MHD: Effects of thermal diffusion and diffusion thermo on free convective heat and mass transfer over a stretching surface considering suction or injection, *Commun. Nonlinear Sci. Numer. Simul.*, **14**, pp. 2202–2214, 2009.

22. A.A. Afify, Some new exact solutions for MHD aligned creeping flow and heat transfer in second grade fluids by using Lie group analysis, *Nonlinear Anal., Theory Methods Appl., Ser. A, Theory Methods*, **70**, pp. 3298–3306, 2009.

23. T. Tapanidis, Gr. tsagas, H.P. Mazumdar, Application of scaling group of transformations to viscoelastic second grade fluid flow, *Nonlinear Funct. Anal. Appl.*, **8**, pp. 345–350, 2003.

24. T.Y. Na, *Computational Methods in Engineering Boundary Value Problems*, Academic Press, New York, 1979.

25. L.J. Crane, Flow past a stretching plate, *Z. Angew. Math. Phys.*, **21**, pp. 645–647, 1970.

26. T.R. Mahapatra, A.S. Gupta, Heat transfer in stagnation point flow towards a stretching sheet, *Heat Mass Transfer*, **38**, pp. 517–521, 2002.

27. R. Nazar, N. Amin, D. Filip, T. Pop, Heat Unsteady boundary layer flow in the region of the stagnation point on a stretching sheet, *Int. J. Eng. Sci.*, **42**, pp. 1241–1253, 2004.